reconstruction to correct the imperfections in the backprojection. Consequently the reconstruction is constrained to best fit the original projections. The comparison operation is repeated iteratively until the optimal solution is found. Especially in the SIRT algorithm, all of the projections are compared simultaneously.

Visualization of the tomograms was carried out using Amira 2.0 software (Visualization Sciences Group). The electron tomography procedures are the same as those adopted by van Poppel et al. (2005) and detailed discussion was given by Friedrich et al. (2005). The samples were prepared using FIB in the same way as those for TEM observation in Chapter 2A, but the final thickness was rather larger, several hundred nanometers for HAADF–STEM tomography.

2B.3 Results

2B.3.1 SEM observation

The outmost layers of all bivalve shells investigated in this study are calcite prismatic structures, in which columnar crystals are surrounded by thick intercrystalline organic walls. Although the prisms of *Pinctada*, *Pteria* and *Atrina* are almost straight, those of *Crassostrea* are inclined at approximately 30° especially in the outer part of the shells (Checa et al., 2009). Figures 2–18, 2–19 and 2–20 show the inner surfaces and cross sections of the prisms in *Pinctada*, *Pteria* and *Crassostrea*, respectively, which were etched by 0.5 M EDTA for 30 minutes. In the case of inner surfaces, the calcite crystals were considerably dissolved owing to the high concentration of EDTA, and

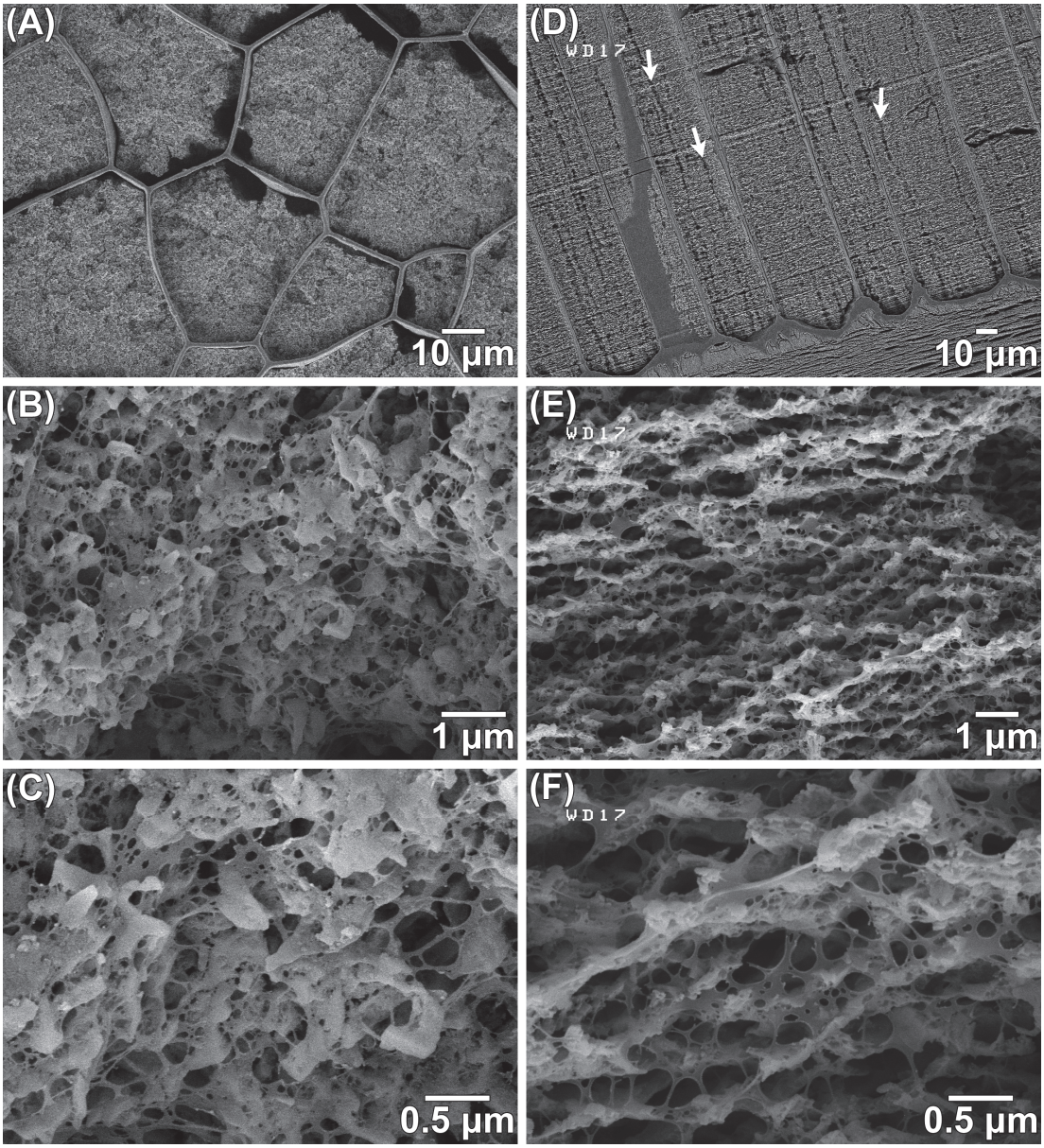

Figure 2–18. SEM images of the prisms in *Pinctada* etched by 0.5 M EDTA for 30 minutes. (A–C) and (D–F) are inner surfaces and cross sections, respectively. Arrows in (D) indicate one of the sinuous grooves that separate the prisms into several domains.

consequently the upper parts of intercrystalline organic walls are exposed on the surfaces because they are EDTA-insoluble (Figures 2–18A, 2–19A and 2–20A).

Also inside the organic walls, *Pinctada* contains fibrous organic networks

(Figure 2–18B) that were similar to the materials reported by Nudelman et al. (2007). The fibrous networks, and partly membranes, of OMs spread out in the crystals (Figure 2–18C). In the cross-sectional observation, sinuous grooves, which separate the prisms into several domains, appeared inside the prisms (Figure 2–18D). The intracrystalline insoluble OMs are distributed vaguely parallel to the shell surfaces in the enlarged view (Figure 2–18E). Both organic networks and membranes were observed also in the cross section (Figure 2–18F).

On the other hand, major components in *Pteria* and *Crassostrea* are membrane-shaped insoluble OMs, which are parallel to the shell surfaces (Figures 2–19B and 2–20B). In their enlarged images, the membranous OMs are holey, not perfect films (Figures 2–19C and 2–20C). TEM observation in Chapter 2A revealed that intracrystalline OMs in the prisms of *Pteria* and *Crassostrea* are located in the direction perpendicular to the *c*-axes, or parallel to the shell surfaces (Figures 2–11B and 2–12B). These outcomes of TEM are consistence with those of SEM in this chapter. Furthermore, the array of intracrystalline OMs is discontinuous in the under-focused TEM images, which is probably because holey-membranous OMs were sliced off when electron-transparent thin specimens of just a few hundred nanometers were prepared using FIB. Hence the holey membranous shapes in SEM images are comparable with those of the intracrystalline OMs in TEM images, and they are not a result of the contraction of OMs due to drying, but an original form inside the crystals. The cross-sectional images confirm that the prisms of *Pteria* are perpendicular to the shell surfaces and those of *Crassostrea* are slightly inclined as mentioned above (Figures 2–19D and 2–20D). The membranous insoluble OMs are distributed parallel to the shell surfaces inside the prisms in the same manner as those observed on inner surfaces

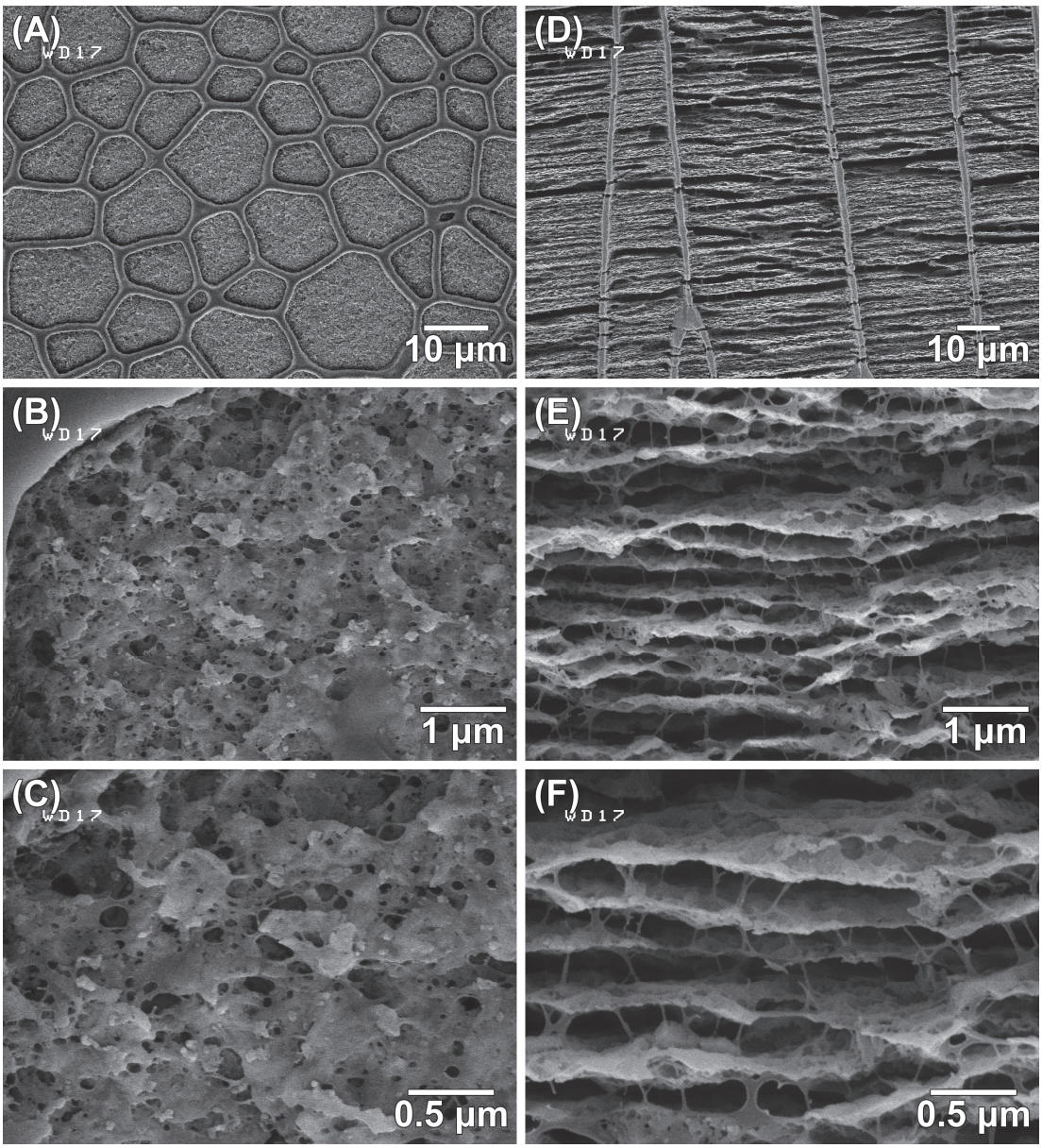

Figure 2–19. SEM images of the prisms in *Pteria* etched by 0.5 M EDTA for 30 minutes. (A–C) and (D–F) are inner surfaces and cross sections, respectively.

(Figures 2–19E and 2–20E). Furthermore, fibrous OMs exist between the membranous OMs and connect the membranes in *Pteria*, which appears to form frameworks like nacreous structures (Figure 2–19F). Although the boundaries between organic membranes are obscure in *Crassostrea*, fibrous OMs were observed between the

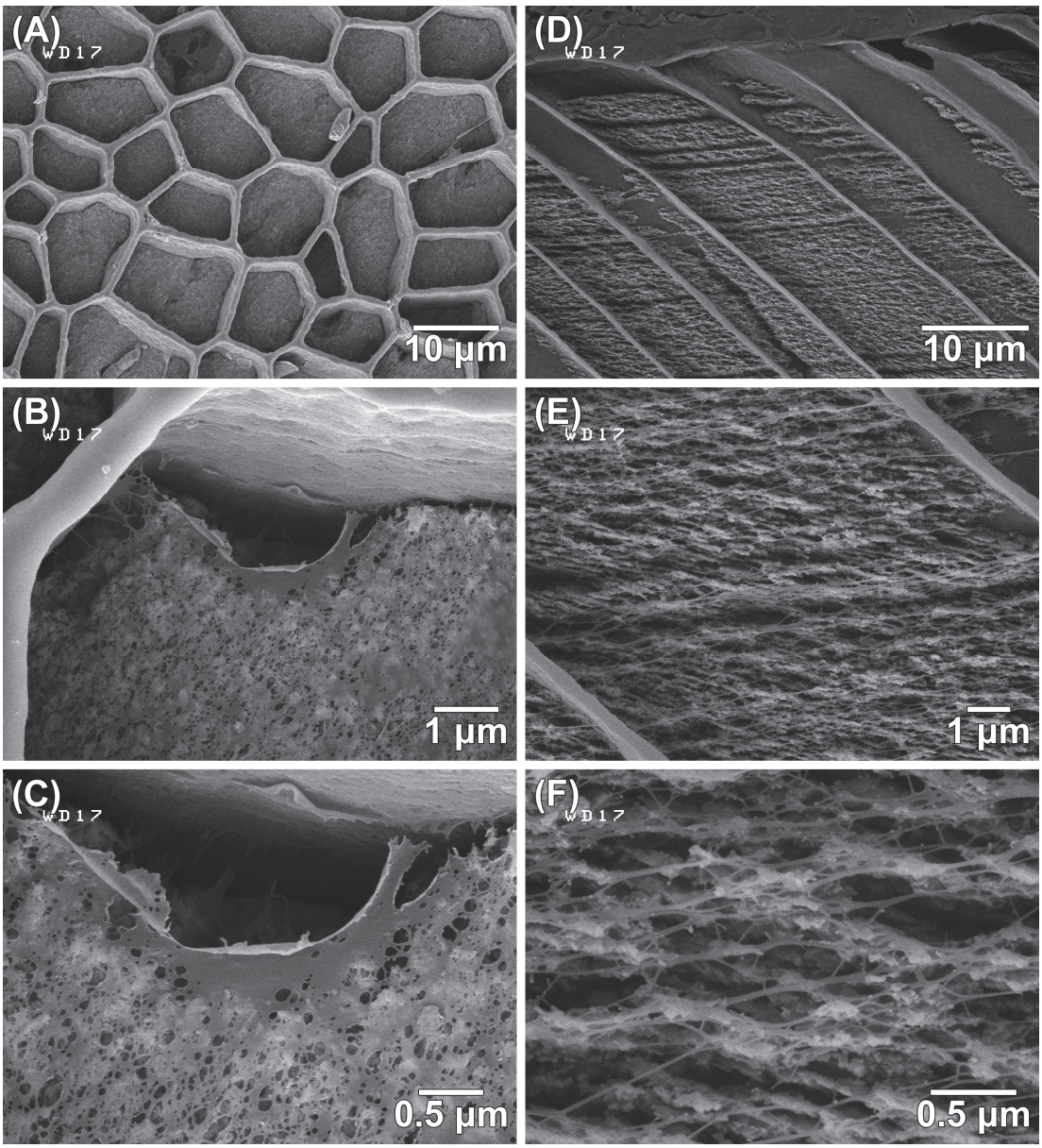

Figure 2–20. SEM images of the prisms in *Crassostrea* etched by 0.5 M EDTA for 30 minutes. (A–C) and (D–F) are inner surfaces and cross sections, respectively.

membranes in places (Figure 2–20F).

The gastropod shells investigated in this study have more complicated layered structures than the bivalve ones. *Haliotis* shells are composed of three-layered structures: superficial aragonite prismatic structure; calcite composite prismatic

structure; and aragonite nacreous structure from the outer surfaces of the shells (Figure 2–21A; Dauphin et al., 2005). The calcite composite prisms in *Haliotis* are not separated by thick organic walls like the prisms in the bivalve shells. In the cross sections etched by 0.5 M EDTA, holey membranous insoluble OMs were observed inside the prisms (Figure 2–21B). Characteristic distribution of membranous OMs like *Pteria* and *Crassostrea* was not found in *Haliotis*, but both bivalve and gastropod shells hold similarly shaped insoluble OMs inside crystals. *Collisella* shells have five layers termed M + 3, M + 2, M + 1, M, and M − 1 (Suzuki et al. 2010). Only M + 3 layer consists of

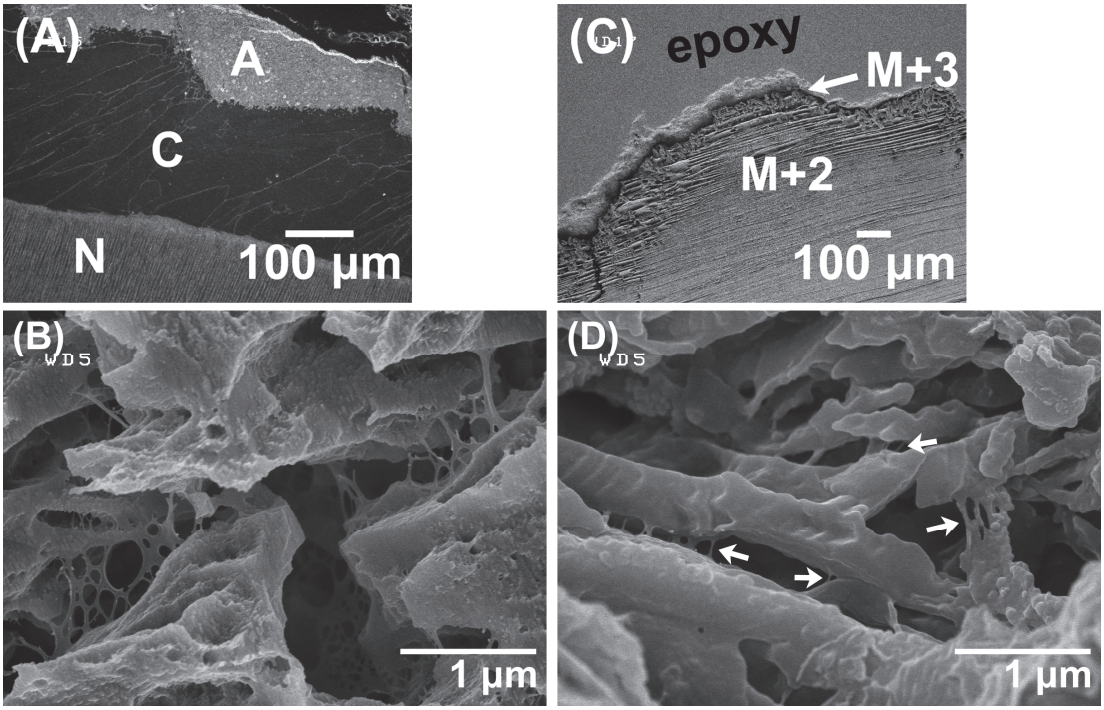

Figure 2–21. SEM images of the cross sections of *Haliotis* and *Collisella*. (A) Low-magnification image of *Haliotis*. A, C and N indicates aragonite prismatic structure, calcite prismatic structure and aragonite nacreous structure, respectively. (B) High-magnification image of *Haliotis* etched by 0.5 M EDTA for 30 minutes. (C) Low-magnification image of *Collisella*. M + 3 and M + 2 layers are shown. (D) High-magnification image of *Collisella* etched by 0.5 M EDTA for 30 minutes. Arrows indicate insoluble OMs.